Title
THE DROPLET MODEL ATOMIC MASS PREDICTIONS

Author
Myers, William D.

Publication Date
1975-10-01

Submitted to Atomic Data and Nuclear Data Tables

LBL-4332
Preprint c.1

THE DROPLET MODEL ATOMIC MASS PREDICTIONS

William D. Myers

October 1975

Prepared for the U. S. Energy Research and Development Administration under Contract W-7405-ENG-48

Submitted to Atomic Data and Nuclear Data Tables LBL-4332

The Droplet Model Atomic Mass Predictions*

William D. Myers

Lawrence Berkeley Laboratory
University of California
Berkeley, California 94720

The motivation behind the development of the Droplet Model is presented along with the atomic mass formula that results. The values of the coefficients appearing in this formula, which were determined by fitting to masses, deformations and fission barriers, are also given. A comparison is made between the measured values of a number of different nuclear properties and the corresponding Droplet Model predictions.

*Work supported by the U. S. Energy Research and Development Administration.

CONTENTS

I. INTRODUCTION

The development of the Droplet Model was begun in 1965 in an attempt to resolve a discrepancy that we had become aware of in the course of preparing an atomic mass table using a more or less conventional Liquid Drop Model (LDM) expression.[1] We had adjusted the coefficients to obtain the best agreement between the predictions of the formula and the measured values of; 1) The atomic masses (which had first been corrected for shell effects using a method developed by Swiatecki[2]) and 2) The fission barriers of a number of heavy nuclei. The inclusion of fission barriers in the fitting procedure is essential for breaking the substantial correlation which otherwise exists between the surface energy coefficient a_2 and the nuclear radius constant r_0.[1] Since we felt that these quantities had been determined quite accurately, the fact that our value of r_0 differed by 8% from the value obtained in electron scattering experiments[3] was seen as a serious discrepancy. A difference like this might have been due to the neglect of higher order terms in the LDM. To see if this was the case we undertook to remove the constraints on the radii of the neutron and proton density distributions that exist in the LDM and to include higher order terms in $A^{-1/3}$ and I^2, where $I = (N-Z)/A$.

The Droplet Model that resulted[4,5] from our work is presented in the next section along with the values of the coefficients determined by fitting to masses and fission barriers. The model not only predicts these macroscopic nuclear properties, but it also may be applied to predictions of nuclear radii, isotope shifts, the neutron skin thickness[6] and even to the prediction of nuclear potential well parameters.[7] The radius constant discrepancy seems to have been resolved since the radii predicted by the Droplet Model are now in good agreement with the measured values.

II. THE MASS FORMULA

The formula employed for predicting the atomic mass excess is the following:

$$\text{Mass Excess} = M_N \cdot N + M_H \cdot Z + \text{Droplet Model Term}$$
$$+ \text{Shell Correction} + \text{Even-Odd Term} + \text{Wigner Term} \qquad (1)$$
$$- 0.00001433 \cdot Z^{2.39}\ \text{MeV}.$$

The coefficients of the first two terms are the mass excesses of the neutron and the hydrogen atom, which have the values[8]

$$M_N = 8.07169\ \text{MeV},$$
$$M_H = 7.28922\ \text{MeV}.$$

The last term is a small correction for the binding of the atomic electrons.[9]

A. Droplet Model Term

The Droplet Model expression is derived in Refs. 4 and 5 and the form employed here is similar to the ones given there,

$$E(N,Z;\text{shape}) = \left[a_1 + J\bar{\delta}^2 - \frac{1}{2}K\bar{\varepsilon}^2 + \frac{1}{2}M\bar{\delta}^4\right]A$$
$$+ \left[a_2 + \frac{9}{4}(J^2/Q)\,\bar{\delta}^2\right]A^{2/3}B_s + a_3A^{1/3}B_k \qquad (2)$$
$$+ c_1Z^2A^{-1/3}B_c - c_2Z^2A^{1/3}B_r - c_3Z^2A^{-1} - c_4 2^{-1/3}Z - c_5Z^2B_w$$

where

$$\bar{\delta} = \left[I + \frac{3}{16}(c_1/Q)\ \ ZA^{-2/3}B_v\right] \Big/ \left[1 + \frac{9}{4}(J/Q)A^{-1/3}B_s\right]$$
$$\qquad (3)$$
$$\bar{\varepsilon} = \left[-2a_2A^{-1/3}\,B_s + L\,\bar{\delta}^2 + c_1\,Z^{\,2}A^{-4/3}B_c\right] \Big/ K.$$

The quantities B_i are the various shape dependencies that enter the formula.[5] As usual they have the value unity for a spherical shape but must be varied both in the search for the ground state deformation and for the fission barrier.[10]

The coefficients appearing in eqs. (2-3) and the values that have been chosen for them are:

$$
\begin{aligned}
a_1 &= 15.960 \text{ MeV, the volume energy coefficient,} \\
a_2 &= 20.69 \text{ MeV, the surface energy coefficient,} \\
J &= 36.8 \text{ MeV, the symmetry energy coefficient,} \\
r_o &= 1.18 \text{ fm, the nuclear radius constant,}
\end{aligned}
\tag{4}
$$

and

$$
\begin{aligned}
a_3 &= 0 \text{ MeV, the curvature correction coefficient,} \\
Q &= 17 \text{ MeV, the effective surface stiffness,} \\
K &= 240 \text{ MeV, the compressibility coefficient,} \\
L &= 100 \text{ MeV, the density-symmetry coefficient,} \\
M &= 0 \text{ MeV, the symmetry anharmonicity coefficient}
\end{aligned}
\tag{5}
$$

The five Coulomb coefficients that appear are defined in terms of the coefficients above, by the expressions:

$$
\begin{aligned}
c_1 &= \frac{3}{5}\,(e^2/r_o) \\
&= 0.73219 \text{ MeV, the Coulomb energy coefficient,}
\end{aligned}
\tag{6}
$$

where $e^2 = 1.4399784$ MeV fm is the square of the electronic charge,

$$
\begin{aligned}
c_2 &= (c_1^2/336)\ (1/J + 18/K) \\
&= 0.00016302 \text{ MeV, volume redistribution coefficient,} \\
c_3 &= \frac{5}{2}\,c_1\ (b/r_o)^2 \\
&= 1.28846 \text{ MeV, diffuseness correction coefficient,}
\end{aligned}
\tag{7}
$$

where b = 0.99 fm is a measure of the diffuseness of the nuclear surface,

$$c_4 = \frac{5}{4}\left(\frac{3}{2\pi}\right)^{2/3} c_1$$

$$= 0.55911 \text{ MeV, exchange correction coefficient,} \qquad (8)$$

$$c_5 = \frac{1}{64}\left(c_1^2/Q\right)$$

$$= 0.00049274 \text{ MeV, surface redistribution coefficient.}$$

The values of a_1, a_2, a_3, J, Q and r_o were determined by fitting to masses and fission barriers, the coefficients K, L and M having been set at what seemed to be physically reasonable values. The coefficient a_3 was found to be poorly determined (it was usually small and either positive or negative depending on what assumptions were made about the other coefficients) and so it was arbitrarily set to zero.

B. Shell Corrections

The shell corrections employed were the same as in our original work[1,2], with the slight modification in shape dependence added in Ref. 11. These references discuss the physical motivation behind the expressions which were used here, and Ref. 12 discusses the details of how the more complicated shape dependence of the Droplet Model was included in the search for ground state deformations.

For the three adjustable parameters that appear in the shell correction we have chosen to retain the values used earlier,[11]

$$C = 5.8 \text{ MeV},$$

$$c = 0.325, \qquad (9)$$

$$a/r_o = 0.444 .$$

In the actual fit, an entirely empirical function F (N or Z) similar to the one given in Section 7.3 of Ref. 1 was employed for N,Z < 20.

C. Even-Odd Term

The even-odd correction term employed here allows for the fact that the separation between the odd and odd-A mass surfaces is slightly smaller than the separation between the even and odd-A surfaces (see the caption to Fig. 2-5 in Ref. 13, for example).

$$\text{Even-Odd Term} = \begin{cases} (\Delta - \tfrac{1}{2}\delta) & \text{odd} \\ (\tfrac{1}{2}\delta) & \text{odd-A} \\ -(\Delta - \tfrac{1}{2}\delta) & \text{even} \end{cases} \quad , \text{ where} \tag{10}$$

$$\Delta = 12/\sqrt{A} \qquad \text{and} \qquad \delta = 20/A \tag{11}$$

D. Wigner Term

There is a vee-shaped through in the nuclear mass surface (see Ref. 1, Section 7.2, for example) that is not a shell-effect in the usual sense. Nor is it an even-odd effect of the type mentioned in the previous section. A term of this kind in the mass equation, proportional to $|I|$, was first discussed by Wigner. (See Ref. 14 and references there to the original works.) The form adopted for our "Wigner term" is

$$E_{Wigner} = W(|I| + \Delta) \quad , \text{ where} \tag{12}$$

$W = 30$ MeV, and

$$\Delta = \begin{cases} 1/A \text{ for odd-odd, } N = Z \text{ nuclei} \\ \text{zero otherwise.} \end{cases} \tag{13}$$

The second term in the brackets of eq. (12) has a similar origin to the leading term[12], and we have chosen to retain it because it is clearly called for by the experimental masses (see Ref. 15, Table I).

III. COMPARISON WITH EXPERIMENT

The Droplet Model coefficients given in the last section were determined by fitting the mass formula to ground state masses and fission barriers. To see how well the model works we will, in the next few sections, compare its predictions with the experimental results for beta-stability properties, ground state masses, fission barriers, deformations and radii.

A. Beta-Stability Properties

A useful way of evaluating the quality of a mass formula is to compare its predictions for the valley of beta-stability with the experimental results.[16] We have fitted the quadratic function $M_A = V_A + \frac{1}{2} C_A (Y - Y_A)^2$ to isobaric sequences after first correcting the measured masses for shell effects, the even-odd mass differences, the Wigner term and the binding of the atomic electrons. (M_A is the mass of the nucleus with mass number A, V_A is the minimum value of the isobaric mass parabola for this value of A and C_A is the "stiffness" of the parabola. The quantity $Y = (N - Z)$ and Y_A is the location of the minimum for this mass number.) The same procedure was carried out for the predicted masses and two sets of coefficients were compared.[12] Of course, the agreement is so good that one must view the differences on an expanded scale in order to see what deviations remain. Figure 1 shows these differences as a function of the mass number A. One general feature is that the bottom of the valley of beta-stability inferred from the measured masses generally lies lower than the predicted value, and that the curvature of the parabolas is generally greater than that predicted. These two deviations tend to compensate. In addition note the relatively large excursion of the measured values of V_A away from those predicted in the vicinity $A = 190$. This difference seems to be due to the relatively poor quality of our shell corrections for nuclei at the end of the rare-earth region. Another deviation that is probably due to shell effects is the tendency of the experimental valley of beta-stability to straighten out in the actinide region and not continue to bend away from the $N = Z$ line as is predicted by the model. This tendency shows up as a downward deviation of Y_A in Fig. 1b for $A \geqslant 210$. In our efforts to understand this deviation we tried other sets of shell corrections[17-19] which reduced the discrepancy to varying degrees but none of them eliminated it entirely.

B. Final Mass Differences

Another way of displaying the differences between the experimental masses and the theoretical predictions is to plot the individual mass differences versus the neutron number as is done in Fig. 2. This plot, which should be compared with similar ones in our previous work[1], shows once again how poor our shell correction function is at the end of the rare earth region. The agreement between our shell function and the experimental one is also poor for the heavy elements.

C. Fission Barriers

In Fig. 3a a number of experimental fission barriers and the corresponding ground state masses, both taken relative to the predicted spherical Droplet Model masses, are plotted against the neutron number N. In Fig. 3b, the Droplet Model prediction for the fission barrier is plotted. The difference between experiment and prediction is shown in Fig. 3c. At first we felt that the deviations shown here constituted a serious discrepancy. However, shell effects at the barrier (which are not included in our calculation) are probably responsible for the deviations in the actinide region, and Mosel[20] has pointed out that the deviations for the lighter nuclei may also be due to shell effects.

D. Deformations

As in our previous work[1,11] one of the results of the calculation of shell effects is a prediction of nuclear ground state deformations. During the fitting procedure the calculated values were compared with the experimental ones from ref. 21. Figure 4 shows that there is rough agreement between theory and experiment for nuclei in the rare-earth and actinide regions. The main deviations seem to be associated (as with the mass deviations) with the inability of our shell correction function to adequately portray the behavior of nuclei at the upper end of the rare-earth region.

E. Radii

The Droplet Model parameters chosen to give the best fit for masses and fission barriers also lead to predictions of nuclear charge radii in quite good agreement with experiment. Figure 5 shows that the Droplet Model fit seems to have resolved the discrepancy, mentioned earlier[1], that existed between the nuclear radius constant inferred from a Liquid Drop Model fit to masses, and that obtained from electron scattering measurements of nuclear charge radii. This figure also shows how the effective sharp radii of the neutron and proton distributions are expected to vary for nuclei along beta-stability and how these radii are related to the radius constant r_0.

IV. REMARKS

Comparisons between the predictions of the Droplet Model and the measured values of the various macroscopic nuclear properties show generally good agreement. Most of the deviations that exist seem to be clearly identifiable with the poor quality of the corrections for shell effects. However, some smooth deviations were seen when the beta-stability properties of the theory were compared with the measured values.

Even though the Droplet Model gives about the same quality of fit as simpler LDM mass formulae when nuclei along beta-stability are considered, it is expected to be more accurate for long range extrapolations because of the higher order effects that are included. It is important to remember that the Droplet Model is more than a mass formula. It is a model covering many of the macroscopic aspects of nuclei. Radii, isotope shifts and the thickness of the neutron skin are predicted. The ground state deformation and fission barrier can be calculated and the important shape dependencies can be applied to the calculation of driving forces in heavy-ion collisions. Extensions of the theory permit prediction of potential well parameters, nuclear diffusenesses, and the restoring forces for nuclear collective excitations.

V. ACKNOWLEDGEMENTS

Most of the Droplet Model development was carried out in collaboration with W. J. Swiatecki. Contributions were made by H. von Groote, R. W. Hasse, E. R. Hilf, P. Möller, S. G. Nilsson, J. R. Nix, P. A. Seeger and C. F. Tsang.

VI. REFERENCES

1. W. D. Myers and W. J. Swiatecki, Nucl. Phys. 81 (1966) 1-60
2. W. J. Swiatecki, Proc. Conf. on Nuclidic Masses, Vienna, 1963, ed. by W. H. Johnson, Jr. (Springer-Verlag, Wein-New York, 1964) p. 58
3. H. R. Collard, L. R. B. Elton and R. Hofstadter, in "Nuclear Radii," Vol. 2, group I Landolt-Börnstein, Numerical data and functional relationships in science and technology. (Springer-Verlag, Berlin, 1967)
4. W. D. Myers and W. J. Swiatecki, Ann. Phys. (N.Y.) 55 (1969) 395-505
5. W. D. Myers and W. J. Swiatecki, Ann. Phys. (N.Y.) 84 (1974) 186-210
6. W. D. Myers, Phys. Letters 30B (1969) 451-4
7. W. D. Myers, Nucl. Phys. A145 (1970) 387-400
8. A. H. Wapstra and N. B. Gove, Nuclear Data Tables 9 (1971) 265
9. L. L. Foldy, Phys. Rev. 83 (1951) 397
10. R. W. Hasse, Ann. Phys. 68 (1971) 377-461
11. W. D. Myers and W. J. Swiatecki, Nuclides Far off the Stability Line, Proc. of the Lysekil Symposium, 1966, Arkiv Fysik 36 (1967) 343-352
12. W. D. Myers, Lawrence Berkeley Laboratory Report, "Droplet Model Description of Nuclear Masses, Fission Barriers and Radii", LBL-3428 (1974)
13. A. Bohr and B. R. Mottelson, Nuclear Structure, Vol. I (W. A. Benjamin, Inc., New York, 1969)
14. J. M. Blatt and V. F. Weisskopf, Theoretical Nuclear Physics (John Wiley and Sons, New York, 1952)
15. G. T. Garvey, et al., Rev. Mod. Phys. 41 (1969) 51-580
16. S. Ludwig, et al., Nucl. Phys. A203 (1973) 627-40
17. P. Möller, private communication

18. P. A. Seeger, private communication

19. J. R. Nix, private communication

20. U. Mosel, Phys. Rev. C, 6 (1972) 971

21. K. E. G. Löbner, M. Vetter and V. Hönig, Nucl. Data A7 (1970) 495-564

22. M. Yamada, Prog. Theor. Phys. 32 (1964) 512.

23. T. Kodama, Prog. Theor. Phys. 45 (1971) 1112-1122

FIGURE CAPTIONS

Fig. 1 The difference between the experimental and calculated values of V_A, Y_A and C_A are plotted against mass number A in order to display the remaining deviations. This particularly useful way of displaying the data was inspired by the work of Yamada[22], Kodama[23], and Ludwig et al.[16]

Fig. 2 The experimental and calculated shell effects and their differences are shown as functions of the neutron number. Isotopes of an element are connected by a line. The large negative deviations at the beginning of the periodic table are for nuclei outside of the fit region, which began at A = 10. A small histogram to the right of part (c) shows how the final errors are distributed for nuclei in the fit region.

Fig. 3 Experimental and calculated saddle masses and their differences are plotted against neutron number N.

Fig. 4 Calculated and experimental quadrupole moments for nuclei in the rare-earth and actinide region are plotted against neutron number. The moments plotted are for those even-even nuclei listed in Ref. 21 with the omission of a few points with large errors whose tabulated values differed substantially from those of adjacent nuclei.

Fig. 5 Various quantities characteristic of the radial extent of spherical nuclei are plotted versus the mass number A. The dashed lines labeled N and Z correspond to the Droplet Model predictions for the quantities $(R_N/A^{1/3})$ and $R_Z/A^{1/3})$ for nuclei along the bottom of the valley of beta-stability. The solid line, which is the weighted mean of the neutron and proton lines, represents the value of $(R/A^{1/3})$ for the total nucleon density. The solid dots correspond to the experimental values of $(R_Z/A^{1/3})$ for various spherical nuclei. The error bars of ± .012 fm were chosen to represent the spread in values observed in the tabulated results. Solid triangles indicate the Droplet Model value of $(R_Z/A^{1/3})$ for these same nuclei. For comparison a dot-dashed line is drawn across the figure at 1.18 fm which is the value of r_o determined by the fitting procedure.

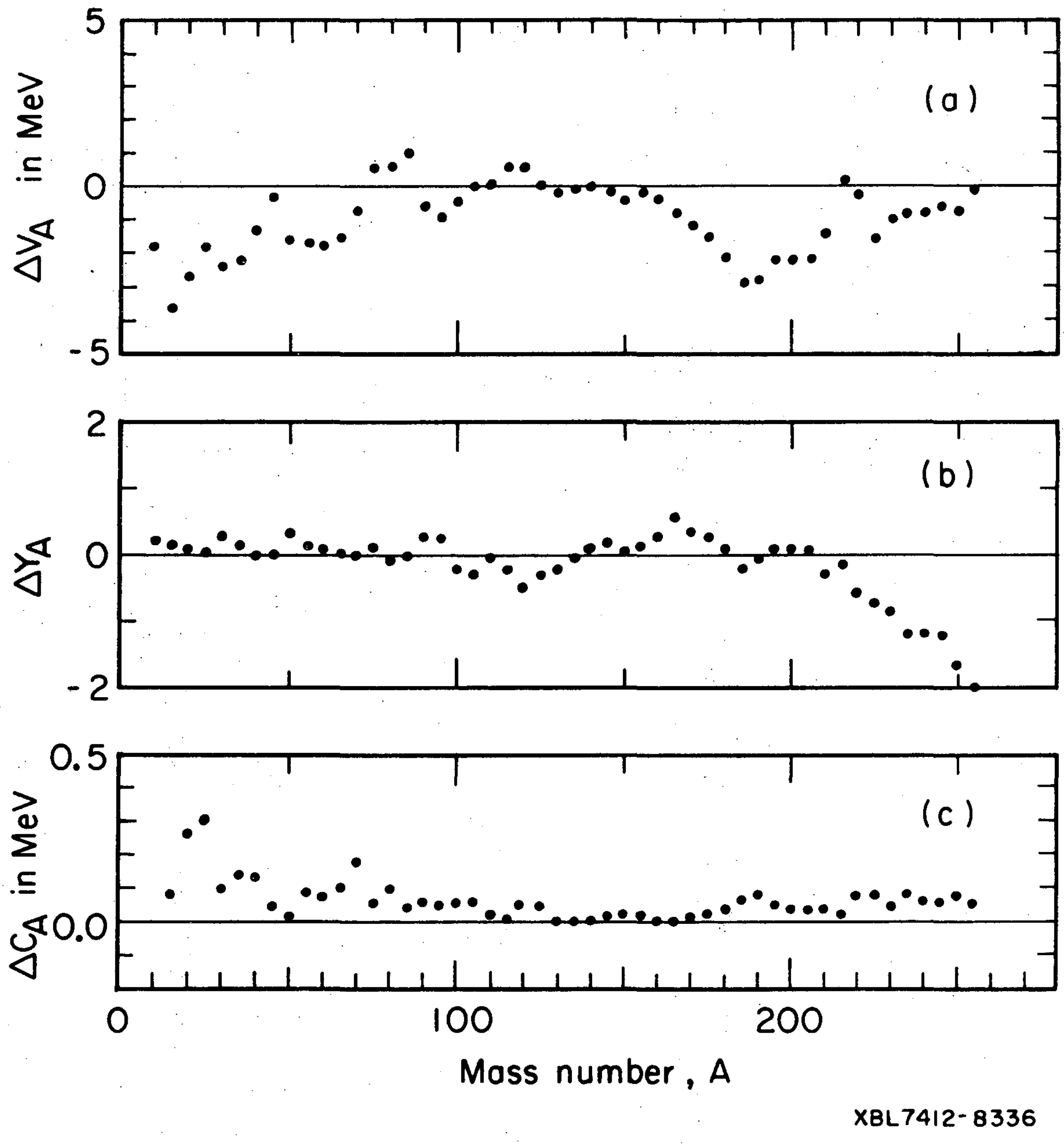
5
0
-5
ΔV_A in MeV
(a)
2
0
-2
ΔY_A
(b)
0.5
0.0
ΔC_A in MeV
(c)
0
100
200
Mass number, A
XBL7412-8336

Fig. 1

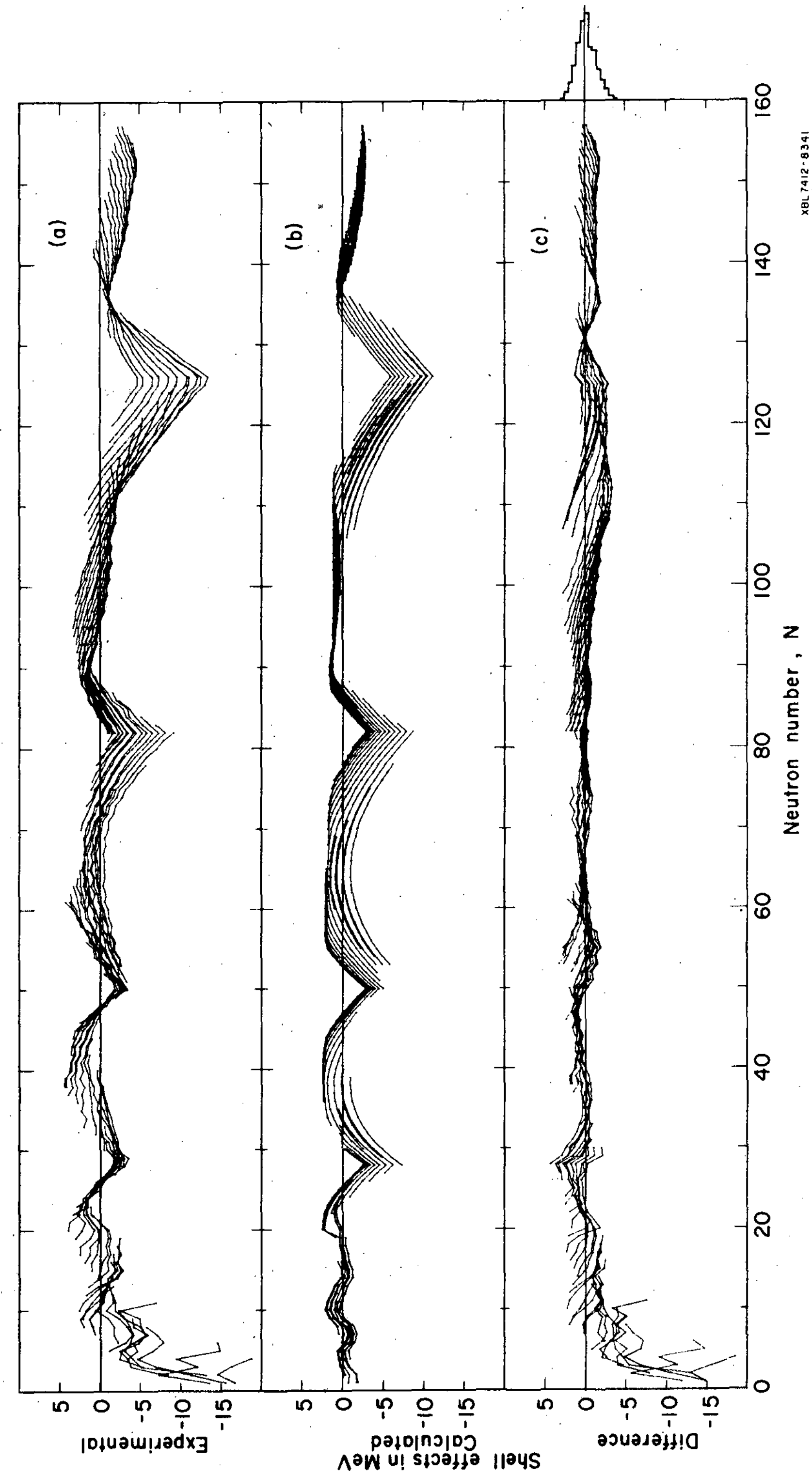
(a)
(b)
(c)
Experimental
Calculated
Shell effects in MeV
Difference
5
0
-5
-10
-15
0
20
40
60
80
100
120
140
160
Neutron number, N
XBL 7412-8341

Fig. 2

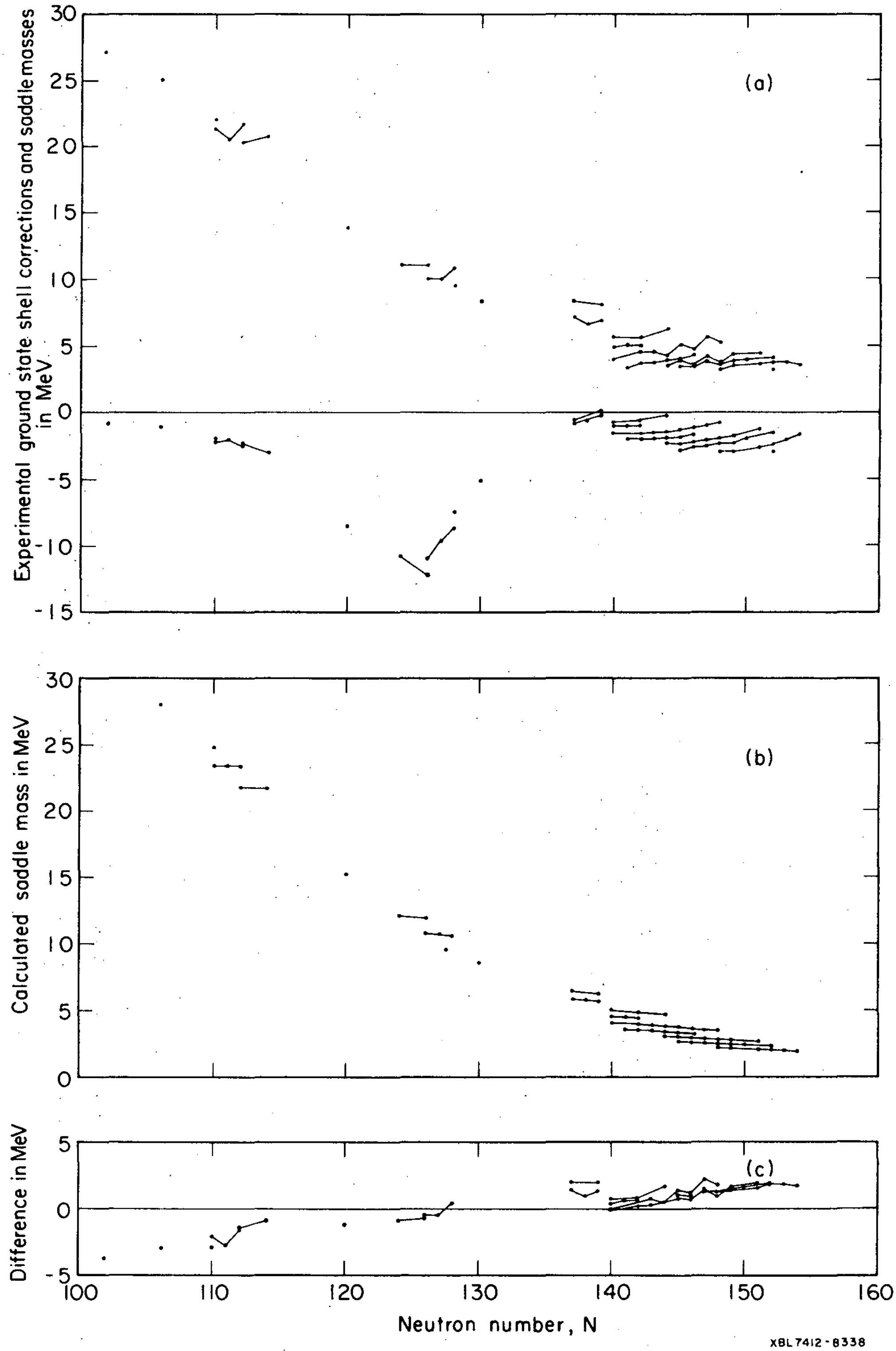
(a)
(b)
(c)
Experimental ground state shell corrections and saddle masses in MeV
Calculated saddle mass in MeV
Difference in MeV
Neutron number, N
30
25
20
15
10
5
0
-5
-10
-15
100
110
120
130
140
150
160
XBL 7412-8338

Fig. 3

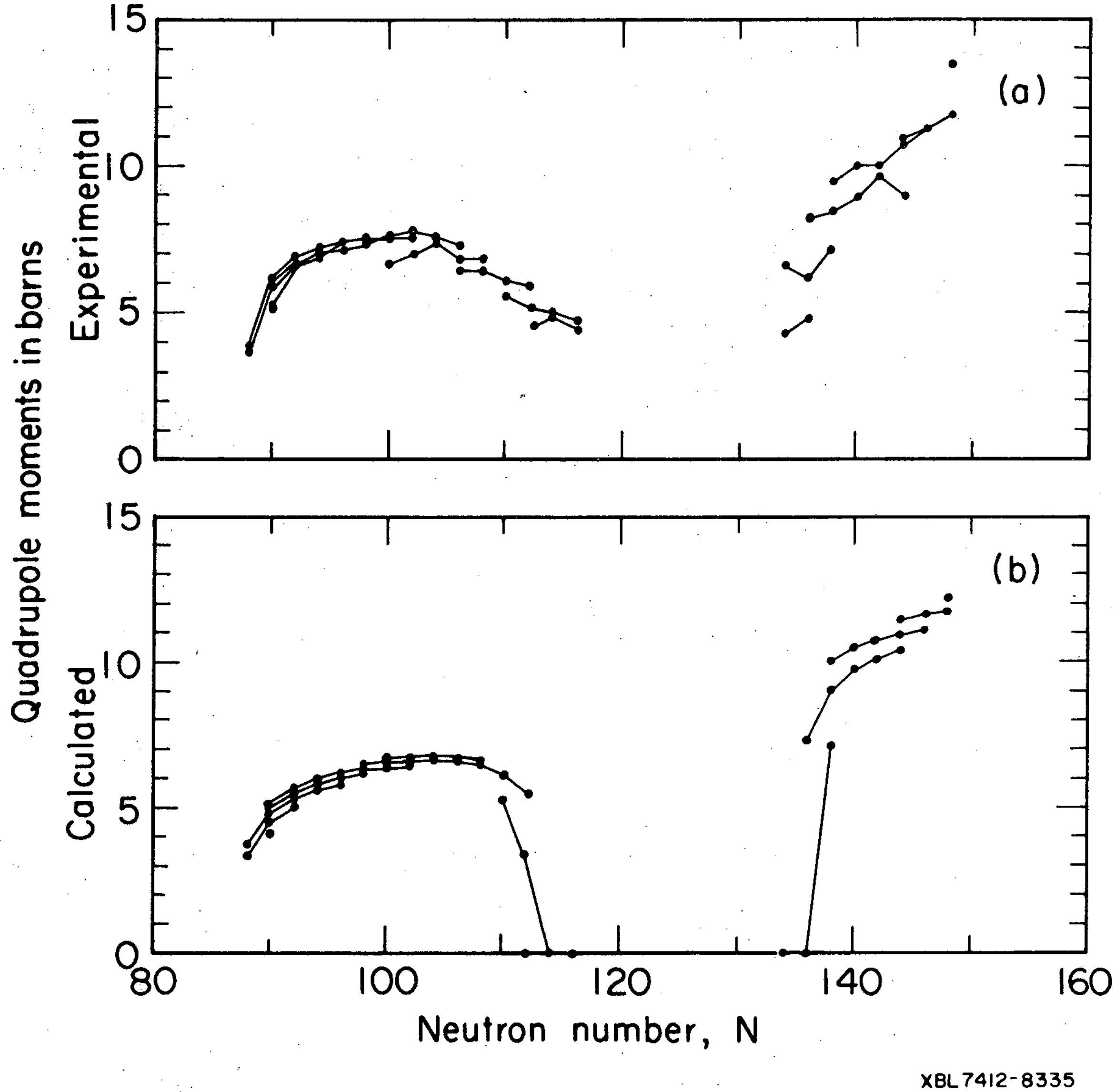

15
10
5
0
(a)
Experimental
Quadrupole moments in barns
(b)
Calculated
80
100
120
140
160
Neutron number, N
XBL 7412-8335

Fig. 4

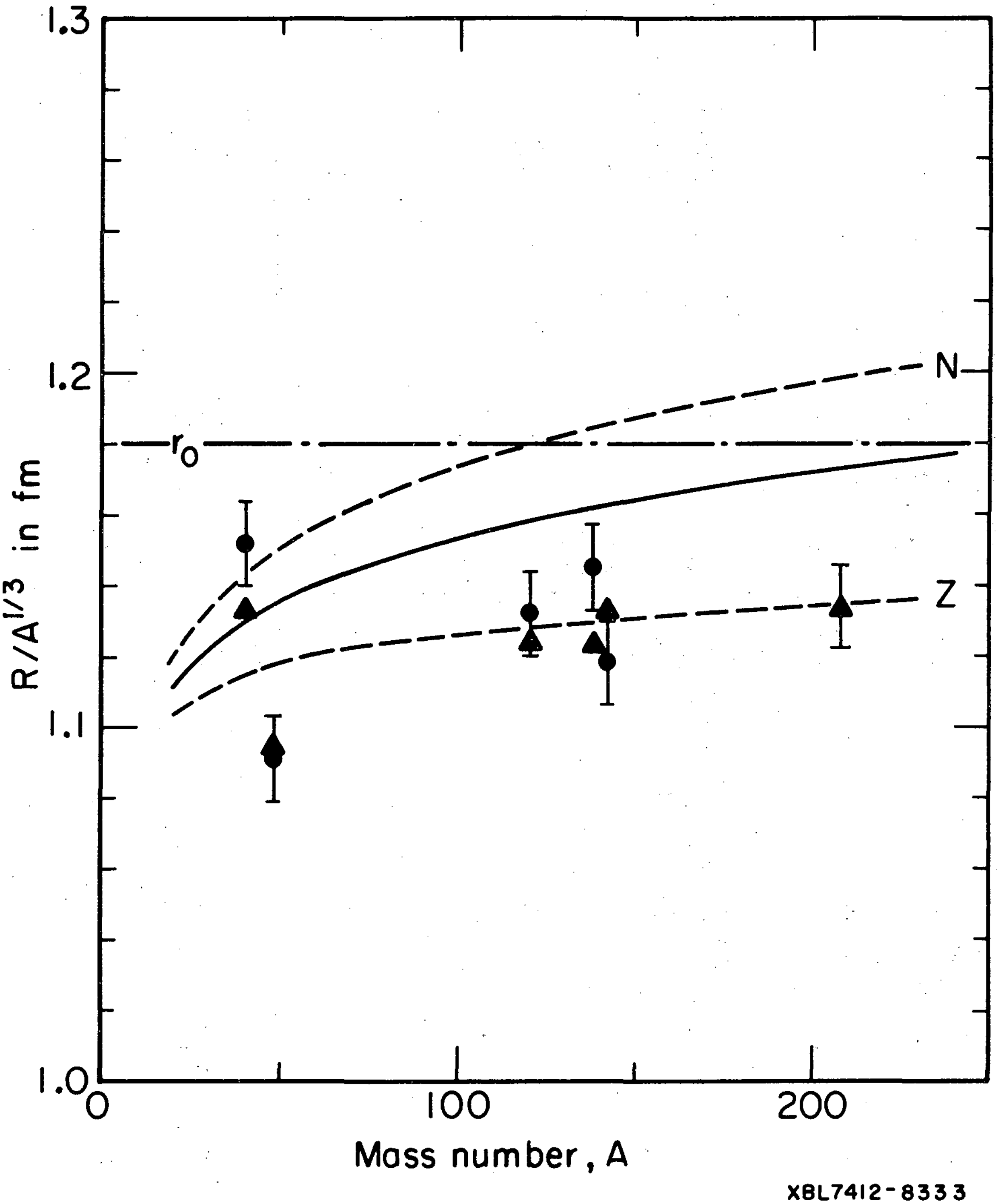

Fig. 5

TECHNICAL INFORMATION DIVISION
LAWRENCE BERKELEY LABORATORY
UNIVERSITY OF CALIFORNIA
BERKELEY, CALIFORNIA 94720